Synthesis and Crystal Structure of Ag_4Br_4 Nanoclusters in the Sodalite Cavities of Fully K^+-Exchanged Zeolite A (LTA)

Woo Taik Lim,[*] Sik Young Choi, Bok Jo Kim,[†] Chang Min Kim,[‡] In Su Lee,[§] Seok Han Kim,[§] and Nam Ho Heo[§,*]

Department of Applied Chemistry, Andong National University, Andong 760-749, Korea. [*]E-mail: wtlim@andong.ac.kr
[†]School of Herb Medicine Resource, Kyungwoon University, Gumi 730-852, Korea
[‡]Department of Chemistry, Kyungpook National University, Daegu 702-701, Korea
[§]Department of Applied Chemistry, Kyungpook National University, Daegu 702-701, Korea
Received May 19, 2005

Ag_4Br_4 nanoclusters have been synthesized in about 75% of the sodalite cavities of fully K^+-exchanged zeolite A (LTA). An additional KBr molecule is retained in each large cavity as part of a near square-planar K_4Br^{3+} cation. A single crystal of Ag_{12}-A, prepared by the dynamic ion-exchange of Na_{12}-A with aqueous 0.05 M $AgNO_3$ and washed with CH_3OH, was placed in a stream of flowing 0.05 M KBr in CH_3OH for two days. The crystal structure of the product ($K_9(K_4Br)Si_{12}Al_{12}O_{48}\cdot 0.75Ag_4Br_4$, a = 12.186(1) Å) was determined at 294 K by single-crystal X-ray diffraction in the space group $Pm\bar{3}m$. It was refined with all measured reflections to the final error index $R_1 = 0.080$ for the 99 reflections for which $F_o > 4\sigma(F_o)$. The thirteen K^+ ions per unit cell are found at three crystallographically distinct positions: eight K^+ ions in the large cavity fill the six-ring site, three K^+ ions fill the eight-rings, and two K^+ ions are opposite four-rings in the large cavity. One bromide ion per unit cell lies opposite a four-ring in the large cavity, held there by two eight-ring and two six-ring K^+ ions (K_4Br^{3+}). Three Ag^+ and three Br^- ions per unit cell are found on 3-fold axes in the sodalite unit, indicating the formation of nano-sized Ag_4Br_4 clusters (interpenetrating tetrahedra; symmetry T_d; diameter *ca.* 7.9 Å) in 75% of the sodalite units. Each cluster (Ag-Br = 2.93(3) Å) is held in place by the coordination of its four Ag^+ ions to the zeolite framework (each Ag^+ cation is 2.52(3) Å from three six-ring oxygens) and by the coordination of its four Br^- ions to K^+ ions through six-rings (Br-K = 3.00(4) Å).

Key Words : Zeolite A, Ag_4Br_4 nanoclusters, Single-crystal X-ray diffraction, Crystal structure

Introduction

Bulk silver halides are unique semiconductors due to their photosensitive properties.[1-3] They are very sensitive to light and may find application as photocatalysts for solar energy conversion and as media for the storage of images or optical information.[4] The incorporation of silver halides into zeolites, which can, due to their regular pore and channel systems, stabilize unusual chemical species including finely dispersed bulk materials, should yield regular arrays of nanosized clusters with quantum-size effects.[1,5,6] Additionally, silver halides in zeolites are known to have photostimulated luminescence (PSL) properties,[7] and these zeolites can be used as image plates for computerized x-ray radiography and as a medium for erasable optical memory.[7]

For these reasons, silver halides in zeolites have been extensively studied as follows. Hirono *et al.*[9] proposed that a silver halide dispersed in a large-pore zeolite could function as an optical recording medium. They synthesized a mordenite (MOR)-AgI inclusion complex by sintering a mixture of mordenite (MOR) and AgI in air at 773 K for about 50 h. Ozin *et al.*[1,10] studied the synthesis, structure, and spectroscopic properties of dispersed silver halide clusters in various halosodalites. Chen *et al.*[4] studied the photostimulated luminescence (PSL) of silver iodide clusters in zeolite Y (FAU). They demonstrated that silver iodide clusters encapsulated in zeolites may work as a medium for erasable optical memory. Kodaira *et al.*[3] discussed the electronic states and structures of the AgI clusters prepared by the direct absorption of bulk AgI into zeolite Na-A. Nanoscale silver iodide guests were also introduced into zeolites Na-ZSM5 (MFI) and Na-Y by Zhai *et al.*[11] who studied their products using XRD, DTA, XPS, and inert-gas adsorption techniques in order to define the placement of the silver iodide. Most of this work focused on AgI in zeolites (direct band gap semiconductor quantum dots),[7-11] rather than AgBr (indirect band gap materials).

Chen *et al.*[12] prepared clusters of AgBr in the size range 30 to 100 Å by a modified reverse micelle synthetic approach and measured their relaxation lifetimes. They confirmed that normally nonemissive indirect band gap materials could become emissive when formulated as small clusters.

To investigate their ionic conductivity, AgBr-montmorillonite composites from 0.9 to 30 volume percent AgBr were studied from 20 to 410 °C by Robledo *et al.*[13] They reported a remarkable increase in the conductivity (about 45 times higher than that of pure AgBr) at 20 °C.

Johansson *et al.*[14] examined the effect of crystallite size on the photophysical properties of silver bromide prepared either in AOT (dioctyl sulfosuccinate, sodium salt) reverse micelle solutions or as gelatin-stabilized dispersions. They found that the principal effect of diminished crystallite size was an enhancement of the indirect exciton emission with a shorter lifetime.

Comor *et al.*[15] prepared 25-Å AgBr quantum dots and studied their room-temperature fluorescence spectra. They were able to assign two bands centered at 340 and 420 nm and discussed the reasons for this emission. (AgBr is normally nonemissive because it is an indirect band gap material.)

While seeking to better understand AgBr-based photography, Ehrlich concluded that a trimer of $AgBr_2^-$, or of $AgBr_3^{2-}$, is the primary nucleus for the absorption peak at 240 nm, with larger clusters being responsible for absorption at longer wavelengths.[16]

In this work, fully Ag^+-exchanged zeolite A (Ag_{12}-LTA) was treated with KBr in CH_3OH solution in an attempt to synthesize nanoclusters of AgBr within the zeolite. The crystal structure of the resulting product was determined to verify that nanoclusters had formed, to learn their positions, size, and geometry, and to observe their interactions with the zeolite framework.

The methods used, and the results, closely parallel those reported earlier for $K_9(K_4I)Si_{12}Al_{12}O_{48}\cdot 0.5Ag_4I_4$.[17]

Experimental Section

Large colorless single crystals of zeolite 4A (LTA), $Na_{12}Si_{12}Al_{12}O_{48}\cdot 27H_2O$ (Na_{12}-A·$27H_2O$ or Na-A), were synthesized by Kokotailo and Charnell.[18] Crystals of hydrated Ag_{12}-A (or Ag-A) were prepared by the dynamic (flow) ion-exchange of Na-A with aqueous 0.05 M $AgNO_3$ (Aldrich 99.998%).[19,20] The resulting Ag-A crystal was thoroughly washed with CH_3OH (Merck 99.8%) and then placed in a flowing stream of 0.05 M KBr (Aldrich 99.9%) in CH_3OH (Merck 99.8%) at 294 K for 2 days. No attempt was made to dry the CH_3OH beforehand. At the end, no attempt was made to remove the solvent from the crystal, neither by evacuation nor heating. The crystal was then isolated in its capillary by sealing both ends with a small torch. The crystal after ion-exchange with Ag^+ was pale reddish brown. After reaction with KBr, it became dark reddish brown.

The structure of the resulting crystal was determined by single-crystal X-ray diffraction techniques at 294(1) K. The cubic space group $Pm\bar{3}m$ (no systematic absences) was used in this work for reasons discussed previously.[21,22] Background intensity was counted at each end of a scan range for a time equal to half the scan time. The intensities of three reflections in diverse regions were recorded every 3 h to monitor crystal and instrumental stability. Only small random fluctuations of these check reflections were observed during the course of data collection. Absorption corrections (μ = 5.13 mm^{-1})[23] were judged to be negligible for this crystal since semi-empirical y-scans showed only negligible fluctuations for several reflections. A summary of the experimental and crystallographic data is presented in Table 1.

Structure Determination

Full-matrix least-squares refinement (SHELXL97)[24] was done on F_o^2 using all data. Refinement was initiated with the atomic parameters of the framework atoms [(Si,Al), O(1), O(2), and O(3)] in dehydrated K_{12}-A.[25] The initial refinement using isotropic thermal parameters for all positions converged to the error indices (defined in footnotes to Table 1) R_1 = 0.43 and R_2 = 0.82.

Refinement including the Ag(1) position at a major peak (0.177, 0.177, 0.177, in the sodalite unit opposite a six-ring) from the initial difference Fourier function led to convergence with R_1 = 0.35 and R_2 = 0.75 and an occupancy of 3.3(2) Ag^+ ions per unit cell. The second largest peak on the subsequent difference Fourier function (based on this model) revealed a peak at (0.232, 0.232, 0.232), opposite a six-ring in the large cavity. Refinement including this peak as K(1) converged to R_1 = 0.30 and R_2 = 0.66, with occupancies of 3.7(2) and 6.4(4) at Ag(1) and K(1), respectively. The addition of another peak at Br(1) (0.038, 0.038, 0.038, inside the sodalite unit) reduced the error indices to R_1 = 0.29 and R_2 = 0.64, with occupancies of 2.5(2), 6.1(3), and 5.4(7) at Ag(1), K(1), and Br(1), respectively. A subsequent refinement including K(2), a peak found near an eight-ring at (0.074, 0.432, 0.5), led to R_1 = 0.28 and R_2 = 0.62, with occupancies of 2.6(2), 7.4(4), 3.7(6), and 2.8(4) for isotropically refined Ag(1), K(1), Br(1), and K(2), respectively. The occupancies at Ag(1) and Br(1) were both fixed at 3.0, an intermediate value, because it appears that Ag_4Br_4 clusters, like those seen before for Ag_4I_4,[17] have formed. The occupancies at K(1) and K(2) were fixed at 8.0 and 3.0, respectively, their maximum values per unit cell. This model converged to R_1 = 0.28 and R_2 = 0.63. A subsequent refinement with anisotropic thermal parameters for all framework atoms [(Si,Al), O(1), O(2), and O(3)] and Ag(1), K(1), and Br(1) converged to R_1 = 0.12 and R_2 = 0.63. A subsequent

Table 1. Summary of Experimental and Crystallographic Data

Crystal cross section (mm)	0.08
Ion exchange for Ag^+ (days, mL)	2, 10.0
Reaction of Ag-A with KBr (days, mL)	2, 10.0
No. of reflections for *a*	15
Range of reflections for *a*	$20^o < 2\theta < 30^o$
Temperature (K)	294(1)
Scan technique	θ-2θ
Scan rate (deg2θ/min)	0.5
Scan width (deg2θ)	0.80 + 0.35 tanθ
$2\theta_{max}$ (deg)	70
Unit cell parameter, *a* (Å)	12.186(1)
No. of unique reflections, *m*	857
No. of reflections with $F_o > 4\sigma(F_o)$	99
No. of variables, *s*	44
Data/parameter ratio, *m*/*s*	19.5
Weighting parameters, a/b	0.161 / 6.07
Final error indices	
R_1[a]	0.080
R_2[b]	0.607
Goodness-of-fit[c]	1.21

[a]$R_1 = \Sigma \mid F_o - \mid F_c \mid \mid / \Sigma F_o$; R_1 is calculated using only the 99 reflections for which $F_o > 4\sigma(F_o)$. [b]$R_2 = [\Sigma w(F_o^2 - F_c^2)^2/\Sigma w(F_o^2)^2]^{1/2}$ is calculated using all 857 unique reflections measured. [c]Goodness-of-fit = $(\Sigma w(F_o^2 - F_c^2)^2/(m-s))^{1/2}$.

difference Fourier function based on this model revealed a peak in the large cavity at (0.245, 0.269, 0.5) opposite a four-ring. Refinement including this peak as K(3) with fixed occupancies of 3.0, 8.0, 3.0, and 3.0 at Ag(1), K(1), Br(1), and K(2), respectively, converged to R_1 = 0.088 and R_2 = 0.59, with an occupancy of 3.8(6) at K(3).

A subsequent difference Fourier function based on this model revealed a peak in the large cavity at (0.304, 0.304, 0.5) opposite a four-ring. Refinement including this peak as Br(2) with fixed occupancies of 3.0, 8.0, 3.0, and 3.0 at Ag(1), K(1), Br(1), and K(2) converged to R_1 = 0.086 and R_2 = 0.60, with occupancies of 1.8(5) at K(3) and 0.8(11) at Br(2).

When this model was refined with fixed occupancies of 3.0, 8.0, 3.0, 3.0, 2.0, and 1.0 at Ag(1), K(1), Br(1), K(2), K(3), and Br(2), respectively, it converged to R_1 = 0.085 and R_2 = 0.60.

Considering the observed content of each sodalite unit, three Ag^+ and three Br^- ions on 3-fold axes opposite six of the eight six-rings per unit cell, there must be at least three different kinds of six-rings per unit cell: three with Ag^+ ions at Ag(1), three with Br^- ions at Br(1), and two with neither. There should therefore also be (at least) three kinds of K^+ ions on the other sides of these six-rings, in the large cavity. In agreement with this, the eight K^+ ions at K(1) were refining with unusually elongated thermal parameters, and another 3-fold-axis peak (0.1890, 0.1890, 0.1890) was seen near K(1) in a subsequent difference Fourier function. A refinement with this peak included as K(1') with occupancies varying at K(1) and K(1') converged to R_1 = 0.083 and R_2 = 0.59 with occupancies of 5.0(9) and 2.5(9) at K(1) and K(1'), respectively. A subsequent difference Fourier function did not show any reasonable peaks around K(1) and K(1'), nor around the O(3) framework oxygen position. Extensive attempts to further resolve the K(1) and K(1') positions were unsuccessful.

The largest peak on the subsequent difference Fourier function appeared at (0.363, 0.363, 0.363). After refinement to (0.362(8), 0.362(8), 0.362(8)), it was 2.20(17) Å from K(1) and 2.63(8) Å from K(3), and could represent solvent oxygen atoms. Including it in least-squares refinement allowed the R values to decrease to R_1 = 0.079 and R_2 = 0.60. However, it refined to an occupancy of 2.0(11) which was not significant, so it is not included in the final model.

The final cycles of refinement with occupancies fixed as shown in Table 2 converged to R_1 = 0.082 and R_2 = 0.59 with anisotropic thermal parameters for all framework and non-framework atoms except for Br(2), K(2), and K(3). On the final difference Fourier function, the largest peak appeared at (0.5, 0.5, 0.5) with height 1.7 $e^-/Å^3$, it was not included in the final model because it was too far from any other atom. The O(4) position was seen again but only as a very minor peak. All shifts in the final cycles of refinement were less than 0.1% for the corresponding estimated standard deviations. The final structural parameters are given in Table 2. Selected interatomic distances and angles are given in Table 3.

Fixed weights were used initially; the final weights were assigned using the formula $w = 1/[s^2(F_o^2) + (aP)^2 + bP]$ where $P = [\mathrm{Max}(F_o^2,0) + 2F_c^2]/3$, with a = 0.161 and b = 6.07 as refined parameters (see Table 1). Atomic scattering factors for Ag, Br, K^+, O^-, and $(Si,Al)^{1.75+}$ were used.[26,27] The function describing $(Si,Al)^{1.75+}$ is the mean of the Si^{4+}, Si^0, Al^{3+}, and Al^0 functions. All scattering factors were modified to account for anomalous dispersion.[28,29]

Results and Discussion

Zeolite A Framework. As in the structure of $K_9(K_4I)$-A·0.5Ag_4I_4,[17] the flex of (distortions to) the framework structure of this structure is much more like that of hydrated K_{12}-A[25] than that of dehydrated K_{12}-A[25] (see Table 4). In fact, the framework angles in this KBr complex differ the most, amongst these structures, from those in dehydrated

Table 2. Positional, Thermal, and Occupancy Parameters[a]

	Wyckoff position	x	y	z	U_{11}	U_{22}	U_{33}	U_{12}	U_{13}	U_{23}	Occupancy[b] fixed	Occupancy[b] varied
(Si,Al)	24(*k*)	0	1827(8)	3691(7)	187(65)	208(73)	0	−104(51)	0	0	24[c]	
O(1)	12(*h*)	0	2142(33)	5000[d]	130(221)	430(302)	825(341)	0	0	0	12	
O(2)	12(*i*)	0	2985(18)	2985(18)	393(244)	186(142)	186(142)	−340(170)	0	0	12	
O(3)	24(*m*)	1138(14)	1138(14)	3446(20)	269(110)	269(110)	574(197)	209(108)	209(108)	562(126)	24	
K(1)	8(*g*)	2575(26)	2575(26)	2575(26)	990(214)	990(214)	990(214)	273(253)	273(253)	273(253)	5	5.0(9)
K(1')	8(g)	2131(33)	2131(33)	2131(33)	373(154)	373(154)	373(154)	107(167)	107(167)	107(167)	3	2.5(9)
Ag(1)	8(*g*)	1411(11)	1411(11)	1411(11)	492(61)	492(61)	492(61)	337(85)	337(85)	337(85)	3	2.6(2)
Br(1)	8(*g*)	866(43)	866(43)	866(43)	5966(784)	5966(784)	5966(784)	−695(429)	−695(429)	−695(429)	3	3.7(6)
Br(2)	12(*j*)	2862(75)	2862(75)	5000[d]	938(454)						1	0.8(11)
K(2)	24(*l*)	575(78)	4192(71)	5000[d]	967(382)						3	2.8(4)
K(3)	24(*l*)	2134(78)	2885(79)	5000[d]	151(245)						2	1.8(5)

[a]Positional parameters × 10^4 and thermal parameters × 10^4 are given. Numbers in parentheses are the estimated standard deviations in the units of the least significant figure given for the corresponding parameter. The anisotropic temperature factor is $\exp[-2\pi^2a^{-2}(U_{11}h^2 + U_{22}k^2 + U_{33}l^2 + 2U_{12}hk + 2U_{13}hl + 2U_{23}kl)]$. [b]Occupancy factors are given as the number of atoms or ions per unit cell. [c]Occupancy for (Si) = 12, occupancy for (Al) = 12. [d]Exactly 0.5 by symmetry.

Table 3. Selected Interatomic Distances (Å) and Angles (deg)[a]

	Distances		Angles
(Si,Al)-O(1)	1.641(13)	O(1)-(Si,Al)-O(2)	107.8(17)
(Si,Al)-O(2)	1.653(12)	O(1)-(Si,Al)-O(3)	107.2(12)
(Si,Al)-O(3)	1.648(8)	O(2)-(Si,Al)-O(3)	109.9(10)
		O(3)-(Si,Al)-O(3)	114.6(19)
K(1)-O(3)	2.69(3)		
K(1')-O(3)	2.34(3)	(Si,Al)-O(1)-(Si,Al)	153(3)
K(1')-O(2)	2.985(15)	(Si,Al)-O(2)-(Si,Al)	152.7(23)
Ag(1)-O(3)	2.52(3)	(Si,Al)-O(3)-(Si,Al)	145.5(16)
Ag(1)-O(2)	3.21(3)		
K(2)-O(1)	2.59(9)	O(3)-K(1)-O(3)	95.2(16)
K(2)-O(2)	2.95(7)	O(3)-K(1')-O(3)	116.1(12)
K(3)-O(1)	2.75(9)	O(3)-Ag(1)-O(3)	104.0(9)
K(3)-O(3)	3.10(8)	O(3)-Ag(1)-Br(1)	93.9(7),150.6(3)
Ag(1)-Br(1)	2.93(3)	Ag(1)-Br(1)-Ag(1)	106.6(17)
K(1')-Br(1)	2.67(12)	Br(1)-Ag(1)-Br(1)	61(3)
K(2)-Br(2)	3.22(9)	K(1)-Br(2)-K(2)	87.6(10)
K(1)-Br(2)	3.00(4)	K(1)-Br(2)-K(1)	161(5)
Br(2)-O(1)	3.60(4)	K(2)-Br(2)-K(2)	150(6)
Br(2)-O(2)	3.52(7)	K(1')-Br(1)-Ag(1)	144.0(17)
Ag(1)-K(1)	2.46(6)		
Br(1)···O(2)	3.80(5)		
Br(1)···O(3)	3.18(6)		

[a]The numbers in parentheses are the estimated standard deviations in the units of the least significant digit given for the corresponding parameter.

K_{12}-A.[25]

K^+ Ions. Although there should be three different kinds of six-rings and therefore three different K^+ positions on the 3-fold axes in the large cavity, only the K(1) and K(1') positions with occupancies of 5 and 3, respectively, are found. Each of the eight six-rings per unit cell contains a K^+ ion. Each K^+ ion lies on a 3-fold axis: K(1) is 2.69(3) Å and K(1') is 2.34(3) Å (very different distances) from its three O(3) oxygens (see Table 3). Considering that the sum of the ionic radii of K^+ and O^{2-} is 1.33 + 1.32 = 2.65 Å,[30,31] respectively, the K(1)-O(3) approach distance, 2.69(3) Å, is reasonable, while the K(1')-O(3) distance, 2.34(3) Å, is much shorter than this sum. The K(1) and K(1') ions extend 1.41 and 0.47 Å, respectively, into the large cavity from the (111) planes at O(3) (see Table 5), and make very different angles with O(3), O(3)-K(1)-O(3) = 95.2(16)° and O(3)-K(1')-O(3) = 116.1(12)°.

Table 5. Deviations of Atoms (Å) from the (111) Plane at O(3)[a]

	$K_9(K_4Br)$-A·0.75Ag_4Br_4[b]	$K_9(K_4I)$-A·0.5Ag_4I_4[c]	Dehydrated K_{12}-A[d]
K(1)	1.41	1.48	0.79
K(1')	0.47	0.55	–
Ag(1)	−1.05	−0.98	–
X(1)[e]	−2.20	−2.17	–

[a]A positive deviation indicate that the ion lies in the large cavity. A negative deviation indicates that the ion lies on the same side of the plane as the origin, *i.e.*, inside the sodalite unit. [b]This work. [c]Reference 17. [d]Reference 25. [e]X = Br or I.

Three K^+ ions at K(2) occupy the three eight-rings per unit cell. Each lies 0.70 Å from its eight-ring plane. Each K(2) ion is 2.59(9) Å from two O(1) oxygens and 2.95(7) Å from an O(2) oxygen of an eight-ring (see Figure 1). Similar unequal coordination of eight-ring oxygens to eight-ring K^+ ions, perhaps with a lesser degree of inequality, was seen in the crystal structures of $K_9(K_4I)$-A·0.5Ag_4I_4,[17] and in hydrated and dehydrated K_{12}-A.[25]

Two K^+ ions per unit cell are found at the K(3) position, opposite four-rings in the large cavity (see Figure 1), as in the crystal structure of $K_9(K_4I)$-A·0.5Ag_4I_4.[17] This position was not found in hydrated nor dehydrated K_{12}-A.[25] Each is 2.75(9) Å from two O(1) oxygens.

The Ag_4Br_4 Nanocluster in the Sodalite Unit. Three Ag^+ ions and three Br^- ions per unit cell occupy nonequivalent 3-fold-axis positions in the sodalite unit. The three Ag^+ ions at Ag(1) lie opposite six-rings in the sodalite unit and the three Br^- ions at Br(1) occupy similar positions, recessed more deeply into the sodalite unit. It is impossible for both a Ag^+ and a Br^- ion to approach the same six-ring because their approach distance, 1.14(11) Å, would be far too short.

The Ag^+ ions at Ag(1) are each 2.52(3) Å from three six-ring oxygens at O(3) (see Table 3) and extend 1.05 Å into the sodalite unit from the (111) planes at O(3) (see Table 5). Considering the ionic radii of the framework oxygens to be 1.32 Å,[30,31] the ionic radii of these Ag^+ ions must be 2.52-1.32 = 1.2 Å. This is very similar to the tabulated ionic radius of Ag^+, 1.13 Å,[30] indicating that it is a Ag^+ ion that is at Ag(1). To achieve charge balance, the bromine positions must be occupied by Br^-.

The three Br^- ions at Br(1) extend 2.20 Å into the sodalite unit from the (111) planes at O(3) (see Table 5). They are thus far (3.18(6) Å, Table 3) from the three nearest anionic framework oxygens, indicating that they are not cations.

Table 4. (Si,Al)-O-(Si,Al) Angles (deg)[a] at Framework Oxygens and Unit Cell Parameters for K^+-Exchanged Zeolite A

K^+-exchanged zeolite A	O(1)	O(2)	O(3)	*a*, Å
Dehydrated K_{12}-A[b]	128.5(6)	178.4(5)	153.7(5)	12.309(2)
Hydrated K_{12}-A[b]	145.2(9)	159.3(6)	146.0(9)	12.301(2)
$K_9(K_4I)$-A·0.5Ag_4I_4[c]	148.5(9)	155.7(8)	143.7(6)	12.290(1)
$K_9(K_4Br)$-A·0.75Ag_4Br_4[d]	153(3)	152.7(23)	145.5(16)	12.186(1)

[a]The numbers in parentheses are the estimated standard deviations in the units of the least significant digit given for the corresponding parameters. [b]Reference 25. [c]Reference 17. [d]This work.

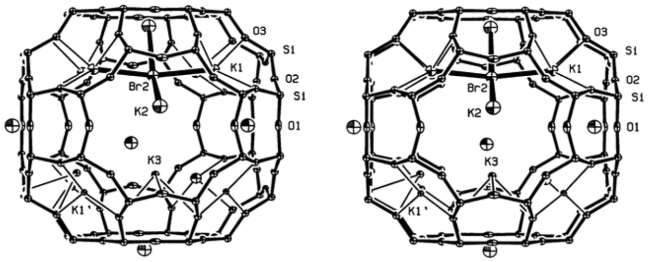

Figure 1. Stereoview of the large cavity of $K_9(K_4Br)$-A·0.75Ag_4Br_4 with an bromide ion bonding to four K^+ ions. Heavy lines indicate K^+-Br^- bonds. The zeolite A framework is drawn with bonds of medium thickness. The coordination of K^+ ions to oxygens of the zeolite framework are indicated by the thinnest lines. Ellipsoids of 20% probability are shown.

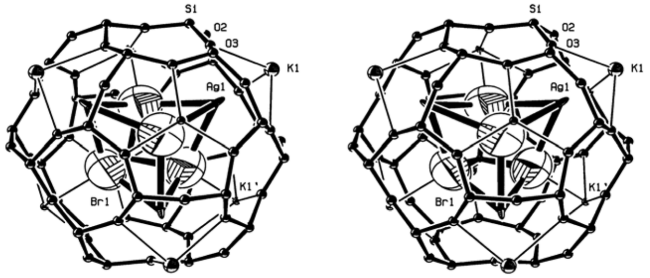

Figure 2. A stereoview of a sodalite unit in $K_9(K_4Br)$-A·0.75Ag_4Br_4. About three-quarters of the sodalite cavities contain a Ag_4Br_4 cluster (heavy lines) as shown. Each Ag^+ cation coordinates octahedrally to three Br(1) iodine ions and to three O(3) framework oxygens. Each bromide ion coordinates tetrahedrally to three Ag^+ ions and to one K^+ ion at K(1'). The coordination of K^+ ions to oxygens of the zeolite framework and to bromide ions are indicated by the thinnest lines. See the caption to Figure 1 for other details.

Furthermore, they approach Ag^+ ions more closely, at 2.93(3) Å, indicating that they are anions; the Ag^+-Br^- bond length in AgBr, 2.88 Å,[32] is similar to that found here. Again, those Br^- ions bond to up to three Ag^+ ions opposite three adjacent six-rings. However, the possible contact distances between Br^- ions within the same sodalite unit are 2.11(10), 2.98(9), and 3.66(8) Å. Considering the occupancy of three Br^- ions at Br(1) per unit cell and the radius of the Br^- ion, 1.96 Å,[30,31] only the latter two approach distances can be considered further. These depend on the occupancies per sodalite unit and their geometric placement.

Considering the possible arrangements of Br^- and Ag^+ ions within the space of the sodalite unit, an interpenetrating tetrahedral (puckered cubic) arrangement of four Ag^+ and four Br^- ions in 75% of the sodalite units is most likely (see Figures 2 and 3). It gives the greatest number of bonds per atom (12 bonds per 8 ions), the most regular coordination geometries (only mildly distorted octahedral for Ag^+ and tetrahedral for Br^-), and is consistent with the symmetry of the Ag(1) and Br(1) positions (both lie on 3-fold axes). In this arrangement, each Ag^+ ion bonds to three Br^- ions (in addition to three framework oxygens), and each Br^- ion bonds to three Ag^+ ions (in addition to one K(1') ion).

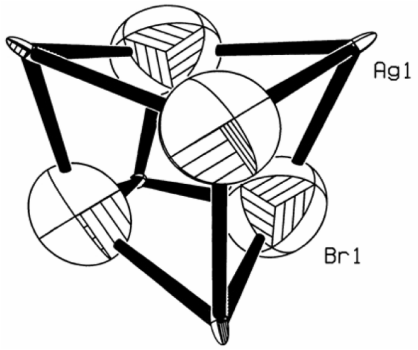

Figure 3. The Ag_4Br_4 cluster (symmetry T_d) found in about three-quarters of the sodalite cavities. See the caption to Figure 1 for other details.

The resulting neutral Ag_4Br_4 nanocluster would be well stabilized by the interactions of each its four Ag^+ ions with three six-ring oxygens (Ag(1)-O(3) = 2.52(3) Å). In addition, each Br^- ion coordinates to a K(1') cation through a six-ring. The stereoview of such a sodalite unit with a Ag_4Br_4 nanocluster at its center is shown in Figure 2.

The Ag_4Br_4 cluster has a diameter of *ca.* 7.9 Å. It is a neutral ionic nanocluster which, like others reported earlier,[1-6,17] may have interesting optical properties. Silver halide clusters of Ag_nX, X = Cl, Br, and I,[1,10] were reported by Ozin *et al.*; each has a halide anion at its center.

A quarter of the sodalite cavities in the crystal are empty (see Figure 4). Each is surrounded by eight K^+ ions at K(1). This material (the zeolite framework, the cations, and the clusters) appears to be stoichiometric, suggesting that this or a similarly prepared material would have very well defined physical properties (see Figure 5). The single crystal studied, a cube about 80 mm on an edge, contained more than 200 Tera (2×10^{14}) Ag_4Br_4 clusters.

In a theoretical study of neutral clusters of $(AgBr)_n$, n = 1-9, Marynick *et al.* found the Ag_4Br_4 cluster to be tetrahedral as reported herein.[33] However, they found the Ag^+ ions to be much closer to the center than the Br^- ions, presumably to form weak $Ag^+ \cdots Ag^+$ interactions.[34,35] In this work the Ag^+ ions are very much pulled outward, each to coordinate to three O(3) oxygen atoms of the zeolite framework (see Figures 2 and 3). The difference is large; because of its environment within this zeolite, the cluster is turned inside out. Marynick *et al.* calculate on angle of 110.5° for Br-Ag-

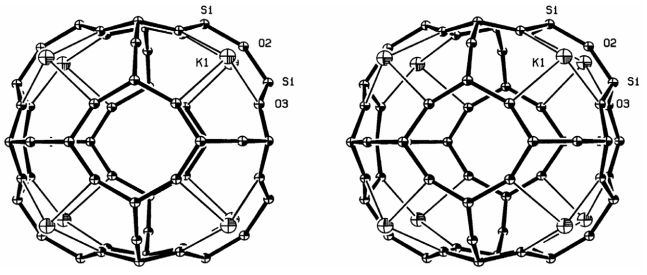

Figure 4. Stereoview of an empty sodalite unit with 8 K(1) K^+ cations. See the caption to Figure 1 for other details.

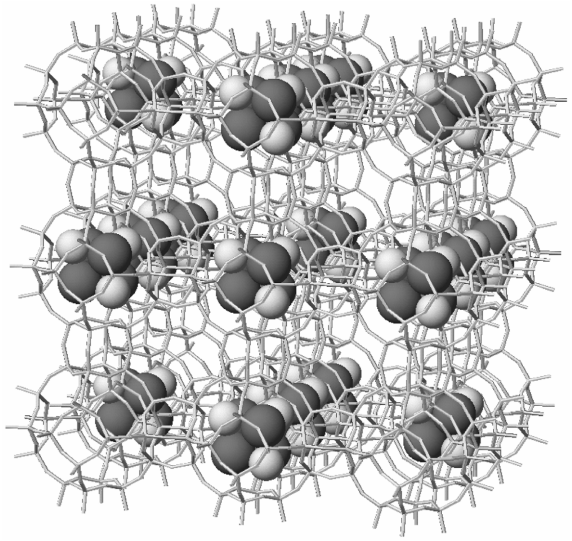

Figure 5. The Ag_4Br_4 clusters in alternating sodalite cavities of several unit cells. For clarity, the framework atoms have been simplified and the K^+ and K_4Br^{3+} cations have been omitted. The long-range ordering and identical orientations of the nanoparticles shown here is reasonable, but it has not been established in this work.

Br whereas 61° is found in this work (Tables 3 and 6; see Figure 3). The corresponding Ag-Br-Ag angles are 64.2° and 106.6°. Their calculated 2.89-Å AgBr bond length agrees with that found here, 2.93(3) Å. More accurate calculations on Ag_nBr_m, n,m ≤ 2 were reported by Rabilloud *et al*.[36]

The K_4Br^{3+} Cluster in the Large Cavity. One bromide ion per unit cell is found at Br(2), on a 2-fold axis opposite a four-ring in the large cavity. It bonds to four K^+ ions, two at K(1) and two at K(2), in a near square-planar manner to give a K_4Br^{3+} cluster (see Figures 1 and 6). Br(2)-K(1) = 3.00(4) and Br(2)-K(2) = 3.22(9) Å; the bond angles about Br(2) can be seen in Table 3. For comparison, the sum of the ionic radii of Br^- and K^+ is 3.29 (= 1.96 + 1.33) Å.[30,31] The bromide ion at Br(2) is recessed *ca*. 0.80 Å from the $K(1)_2K(2)_2$ plane toward the center of the large cavity (see Figure 6). This is probably because of repulsive interactions with the O(1) and O(3) framework oxygens that are only 3.60(4) and 3.52(7) Å away, respectively (see Table 3 and Figure 1). To coordinate to Br(2), the eight-ring K^+ ions at K(2) have moved closer to the anion and out of the planes of their eight-rings. In this way, three K^+ ions have cooperated to capture one KBr molecule per unit cell. Finally, this K_4Br^{3+} cluster has the same formula as the Ag_nX^{n+} clusters found in various halosodalites by Ozin *et al*.;[1,10] it differs by being far from tetrahedral and by not being in a sodalite cavity.

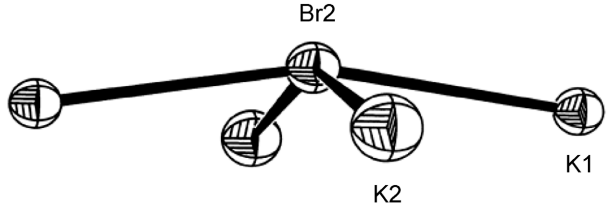

Figure 6. The near square-planar K_4Br^{3+} cation in the large cavity. Ellipsoids of 20% probability are shown.

Table 6. Comparison of the Geometries of the Ag_4Br_4 and Ag_4I_4 Nanoclusters

	Ag_4Br_4[a]	Ag_4I_4[b]
Ag(1)-X(1), Å	2.93(3)	2.973(21)
Ag(1)-X(1)-Ag(1), deg	106.6(17)	112.6(8)
X(1)-Ag(1)-X(1), deg	61(3)	60.5(16)
Ag(1)-O(3), Å	2.52(3)	2.478(11)
X(1)-K(1'), Å	2.67(12)	2.72(6)
X(1)···O(2), Å	3.80(5)	3.80(6)
X(1)···O(3), Å	3.18(6)	3.14(4)
Ag-X, Å in AgX(s)	2.89[c]	3.04[d]

[a]This work. [b]Reference 17. [c]References 37 and 38. AgBr has the NaCl structure with a = 5.7745 Å; both Ag^+ and Br^- are 6-coordinate. [d]Reference 37. AgI adopts the NaCl structure only at elevated pressures. At 1 bar, it has the wurtzite structure; Ag^+ and I^- are both 4-coordinate with Ag-I = 2.81 Å.

Net Reactions. The net reactions that occurred during sample preparation are therefore, in H_2O

$$Na_{12}\text{-}A + 12Ag^+ \rightarrow Ag_{12}\text{-}A + 12Na^+ \quad (1)$$

and, in wet CH_3OH

$$Ag_{12}\text{-}A + 13K^+ + 4Br^- \rightarrow K_9(K_4Br)\text{-}A\cdot 0.75Ag_4Br_4 + 9Ag^+ \quad (2)$$

Comparison of $K_9(K_4Br)$-A·0.75Ag_4Br_4 and $K_9(K_4I)$-A·0.5Ag_4I_4. The positions of the non-framework ions in $K_9(K_4Br)$-A·0.75Ag_4Br_4 are similar to those in $K_9(K_4I)$-A·0.5Ag_4I_4.[17] Table 6 is a compilation of their comparative geometries, which are therefore also quite similar. Although both materials were prepared by the same procedure, the occupancies at the K^+, Ag^+, and X^- (X = Br or I) positions are somewhat different in the two structures. In $K_9(K_4I)$-A·0.5Ag_4I_4,[17] there are six K^+ ions at K(1) and two at K(1'). However, in $K_9(K_4Br)$-A·0.75Ag_4Br_4 there are five at K(1) and three at K(1'). In the Ag_4I_4 complex, half of the sodalite cavities contain an Ag_4I_4 group;[17] for the Ag_4Br_4 inclusion complex, this fraction is about three-quarters.

Summary

Ag_4Br_4 nanoclusters with T_d symmetry have been synthesized in about 75% of the sodalite cavities of K-A by treating Ag-A with KBr in CH_3OH. One KBr molecule per unit cell is retained deep in each large cavity as part of a nearly square-planar K_4Br^{3+} ion.

Acknowledgement. We gratefully acknowledge the support of the Central Laboratory of Kyungpook National University for the diffractometer and computing facilities. This work was supported by Korea Research Foundation Grant (KRF-2002-037-C00017).

Supporting Information Available: Tables of calculated

structure factors squared and observed structure factors squared with esds for $K_9(K_4Br)$-A·0.75Ag_4Br_4 (10 pages) are available from the corresponding author and via the internet at *http://www.kcsnet.or.kr/bkcs*.

References

1. Stein, A.; Ozin, G. A.; Stucky, G. D. *J. Am. Chem. Soc.* **1992**, *114*, 8119.
2. Stein, A.; Ozin, G. A.; Stucky, G. D. *J. Am. Chem. Soc.* **1990**, *112*, 904.
3. Kodaira, T.; Ikeda, T.; Takeo, H. *Eur. Phys. J. D* **1999**, *9*, 601.
4. Chen, W.; Wang, Z.; Lin, Z.; Lin, L.; Fang, K.; Xu, Y.; Su, M.; Lin, J. *J. Appl. Phys.* **1998**, *83*, 3811-3815 and references therein.
5. Srdanov, V. I.; Blake, N. P.; Markgraber, D.; Metiu, H.; Stucky, G. D. *Advanced Zeolite Science and Applications, Studies in Surface Science and Catalysis*; Jansen, J. C., Stocker, M., Karge, H. G., Weitkamp, J., Eds.; Elsevier Science: Amsterdam, 1994; Vol. 85, pp 115-144.
6. Tani, T.; Murofushi, M. *J. Imaging Sci. Technol.* **1994**, *38*, 1.
7. Takahashi, K.; Miyahara, J.; Shibahara, Y. *J. Electrochem. Soc.* **1985**, *132*(6), 1492.
8. Kellerman, R.; Texter, J. *J. Chem. Phys.* **1979**, *70*, 1562.
9. Hirono, T.; Yamada, T. *Japanese Patent 61-061894*, 1986.
10. Godber, J.; Ozin, G. A. *J. Phys. Chem.* **1988**, *92*, 4980.
11. Zhai, Q. Z.; Qiu, S.; Xiao, F. S.; Zhang, Z. T.; Shao, C. L.; Han, Y. *Materials Research Bulletin* **2000**, *35*, 59.
12. Chen, W.; McLendon, G.; Marchetti, A.; Rehm, J. M.; Freedhoff, M. I.; Myers, C. *J. Am. Chem. Soc.* **1994**, *116*, 1585.
13. Robledo, A.; Garcia, N. J.; Bazan, J. C. *Solid State Ionics* **2001**, *139*, 303.
14. Johansson, K. P.; Marchetti, A. P.; McLendon, G. L. *J. Phys. Chem.* **1992**, *96*, 2873.
15. Comor, M. I.; Nedeljkovic, J. M. *Chemical Physics Letters* **1999**, *299*, 233.
16. Ehrlich, S. H. *J. Imaging Sci. Technol.* **1994**, *38*, 201.
17. Heo, N. H.; Kim, H. S.; Lim, W. T.; Seff, K. *J. Phys. Chem. B* **2004**, *108*, 3168.
18. Charnell, J. F. *J. Crystal Growth* **1971**, *8*, 291.
19. Kim, Y.; Seff, K. *J. Phys. Chem.* **1978**, *82*, 1071.
20. Kim, Y.; Seff, K. *J. Am. Chem. Soc.* **1978**, *100*, 6989.
21. Cruz, W. V.; Leung, P. C. W.; Seff, K. *J. Am. Chem. Soc.* **1978**, *100*, 6997.
22. Mellum, M. D.; Seff, K. *J. Phys. Chem.* **1984**, *88*, 3560.
23. *International Tables for X-ray Crystallography*; Kynoch Press: Birmingham, England, 1974; Vol. IV, pp 61-66.
24. Sheldrick, G. M. *SHELXL97*, *Program for the Refinement of Crystal Structures*; University of Gottingen, Germany, 1997.
25. Leung, P. C. W.; Kunz, K. B.; Seff, K.; Maxwell, I. E. *J. Phys. Chem.* **1975**, *79*, 2157.
26. Doyle, P. A.; Turner, P. S. *Acta Crystallogr., Sect. A* **1968**, *24*, 390.
27. *International Tables for X-ray Crystallography*; Ibers, J. A., Hamilton, W. C., Eds.; Kynoch Press: Birmingham, England, 1974; Vol. IV, pp 71-98.
28. Cromer, D. T. *Acta Crystallogr.* **1965**, *18*, 17.
29. *International Tables for X-ray Crystallography*; Kynoch Press: Birmingham, England, 1974; Vol. IV, pp 148-150.
30. Emsley, J. *The Elements*; Oxford University Press: 1990; p 176.
31. *Tables of Interatomic Distances and Configuration in Molecules and Ions*; The Chemical Society: London, 1958.
32. *Comprehensive Inorganic Chemistry*; Bailar Jr., J. C., Emeleus, H. J., Nyholm, Sir R., Trotman-Dickenson, A. F., Eds.; Pergamon Press: 1976; Vol. 3, p 95.
33. Zhang, H.; Schelly, Z. A.; Marynick, D. S. *J. Phys. Chem. A* **2000**, *104*, 6287.
34. Jansen, M. *Angew. Chem. Int. Ed. Engl.* **1987**, *26*, 1098.
35. Choi, E. Y.; Kim, S. Y.; Kim, Y.; Seff, K. *Microporous Mesoporous Mater.* **2003**, *62*, 201.
36. Rabilloud, F.; Spiegelmann, F.; Heully, J. L. *J. Chem. Phys.* **1999**, *111*, 8925.
37. Wells, A. F. *Structural Inorganic Chemistry*, 5th Ed.; Clarendon Press: Oxford, 1984; pp 410-411.
38. *Handbook of Chemistry and Physics*, 80th Ed.; CRC Press: Boca Raton, 1999/2000; p **4**-147.